Ab Initio Benchmark Study of (2-Pyridone)$_2$, a Strongly Bound Doubly Hydrogen-Bonded Dimer

Andreas Müller, Martin Losada, and Samuel Leutwyler*

Departement für Chemie und Biochemie, Universität Bern, Freiestrasse 3, CH-3012 Bern, Switzerland

Received: July 18, 2003; In Final Form: October 15, 2003

The 2-pyridone dimer, $(2PY)_2$, has two antiparallel N−H···O H-bonds analogous to nucleobase dimers. The gas-phase rotational constants and all six intermolecular vibrational frequencies of $(2PY)_2$ have been previously measured, providing benchmarks for theory. The structure, rotational constants, vibrational frequencies, and binding and dissociation energies of $(2PY)_2$ were calculated at the correlated level using second-order Møller−Plesset perturbation theory (MP2) with medium to very large basis sets. The MP2 binding energy limit was extrapolated to the complete basis set (CBS) as $D_{e,CBS} = -22.62 \pm 0.07$ kcal/mol. Higher order correlation energy contributions to D_e at the CCSD(T) level are destabilizing (+0.77 kcal/mol). This implies that $(2PY)_2$ is the most strongly bound doubly hydrogen-bonded dimer known so far. The Hartree−Fock contribution to $D_{e,CBS}$ is only ≈65%. Several medium-size basis sets yield MP2 D_e's within ±5% of the CBS value, as well as structure, rotational constants, and intermolecular vibrations in good agreement with experiment. The PW91 density functional method also shows very good performance with regard to all properties calculated, comparable to MP2. The results imply that correlated methods combined with carefully chosen medium-size basis sets may give near-quantitative results for the structures, binding energies, and intermolecular vibrational frequencies of nucleic acid base dimers.

1. Introduction

Ab initio methods now yield quantitative predictions for the structures and energetics of small hydrogen-bonded gas-phase dimers.[1−7] For larger dimers of biological interest such as nucleobase dimers, the situation is less clear. A number of studies of nucleobase dimers have been performed using the SCF method, usually because correlated methods are too expensive.[8−12] However, SCF calculations predict hydrogen bonds that are too long and binding energies that are too small; increasing the basis set size usually worsens agreement with experiment.[1−3,7,13−15] To reliably calculate dimer structures and binding energies, electron correlation must be included to capture the intermonomer correlation energy as well as changes of intramonomer correlation. In recent years, the MP2 method has been increasingly applied to nucleobase dimers using small and specially designed basis sets.[15−19] More recently, the approximative resolution of the identity MP2 (RI-MP2) method has been applied to the study of H-bonded and stacked nucleobase dimers,[20] as well as advanced correlated methods such as CCSD(T).[21,22] The latter studies addressed mainly the relative binding energies of different nucleobase dimers, using geometries calculated with smaller basis sets. However, MP2 structure optimizations of nucleobase dimers with large basis sets are computationally still very expensive and are often prohibitive for calculations of vibrational frequencies and intensities. The RI-MP2 method does not yet allow to calculate vibrational frequencies.

Two different types of nucleic acid base pairs can exist in the gas phase: near-planar or coplanar structures, which are bound by two or three hydrogen bonds and vertically "stacked" dimers. For the stacked uracil dimer, U·U, MP2 calculations with increasingly large basis sets have established two different isomers, with binding energies of $D_e = 7-10$ kcal/mol.[18,19,23] In the hydrogen-bonded dimers, the intermolecular interactions are nearly always N−H···O═C and N−H···N hydrogen bonds,[24] leading to $D_e = -14$ to -18 kcal/mol,[18] which are larger than the D_e's of the stacked isomers.

The gas-phase dissociation energies D_0 of nucleobase dimers are still not known. The gas-phase base pairing enthalpy of A·T was determined by field ionization mass spectrometry at $T = 350$ K as $\Delta H^\circ_{350} = -13.0$ kcal/mol, and that of G·C as $\Delta H^\circ_{350} = -21.0$ kcal/mol.[25−27] It has now become clear from ab initio calculations[28−30] that the value for the A·T pair most probably refers to a mixture of different isomers, and also that the Watson−Crick and Hoogsteen forms are not among these.

2-Pyridone (2PY) is the simplest aromatic with neighboring N−H and C═O groups and is a hydrogen-bonding analogue of uracil. The $(2PY)_2$ dimer has antiparallel N−H···O hydrogen bonds,[31,32] like most hydrogen-bonded isomers of the uracil dimer U·U.[18] $(2PY)_2$ has been previously studied by different spectroscopic techniques, which have yielded precise rotational constants and N···O hydrogen bond (HB) distances,[32] as well as inter- and intramolecular vibrational frequencies.[13,14,33−35] The availability of accurate gas-phase data allows us to benchmark different methods and basis sets on this doubly hydrogen-bonded dimer. Here, we present a comparative study using as correlated ab initio methods second-order Møller−Plesset perturbation theory (MP2) and two different density functional (DFT) methods, B3LYP and PW91. The basis sets employed range from small and medium Pople-type basis sets up to the augmented correlation-consistent Dunning aug-cc-pVXZ (X = D, T, Q) basis sets. Our aims are

(i) to establish, using complete basis set extrapolations at the MP2 and CCSD(T) levels, an accurate dimer structure and hydrogen bond binding energy D_e;

(ii) to explore, at the MP2 level, whether smaller basis sets can be identified that give near-quantitative predictions of

10.1021/jp0361024 CCC: $27.50
Published on Web 11/26/2003

structural, vibrational, and energetic properties [such information is necessary for the study of larger and nonsymmetric dimers for which large basis sets cannot yet be employed, due to the rapid increase of computational cost with system size ($\approx N$,[5] where N is the number of basis orbitals)];

(iii) to compare the benchmark and other MP2 level results in (i) and (ii) with those of selected DFT methods, which promise effective performance at reduced computational cost.

2. Methods

Correlated calculations of $(2PY)_2$ were performed using the MP2 method. The MP3 and MP4 perturbation theoretical methods in general do not improve the predicted properties of hydrogen-bonded systems.[7] The basis sets include the 6-31G*(0.25) basis set advocated by Hobza et al.[15,16] and the polarized valence double- and triple-ζ basis sets 6-31G(d,p), 6-31+G(d,p), and 6-311++G(d,p); all electrons were correlated. For the complete basis set (CBS) study we employ the double-, triple-, and quadruple-ζ augmented correlation-consistent aug-cc-pVXZ (X = D, T, Q) basis sets of Dunning;[36−38] for these, the core electrons were not correlated (frozen core), because this series of basis sets was optimized with the frozen core MP2 procedure.[36−38]

The properties obtained from MP2 calculations are compared to those of density functional calculations. Tsuzuki and Lüthi have shown that the PW91 functional gives the best potential energy curves and binding energies of six functionals that they tested for both dispersively bound and hydrogen-bonded systems;[39] hence we employ the PW91 functional with the 6-311++G(d,p) basis set. Rabuck and Scuseria have shown that B3LYP/6-311++G(d,p) is well suited for geometries and energies of hydrogen-bonded structures, closely comparable to the Becke "half-and-half" exchange functional (BHLYP) and definitely superior to kinetic-energy dependent functionals.[40] We have previously found good agreement of B3LYP/6-311++G-(d,p) harmonic intermolecular vibrational frequencies with the experimental ones.[13,33] We note that DFT methods are not suggested for the calculation of stacking interactions.[17]

All geometries were fully optimized using analytic gradients without symmetry restrictions and using the most stringent convergence criteria ($<2 \times 10^{-6}\ E_h\ a_0^{-1}$). The same level of theory was used for corresponding geometry optimizations, energy calculations, and (where possible) harmonic frequency analyses. The Boys−Bernardi counterpoise (CP) corrections to the binding energies were calculated as estimates of the basis set superposition error (BSSE).[41,42] In general, MP2 calculations with small to medium basis sets will underestimate the dispersion energy; however, they have larger BSSE contributions that cause them to overestimate the binding energy, so that error compensation often occurs. The B3LYP and PW91 DFT methods exhibit comparatively small BSSEs, typically about 5% of D_e.

Normal mode calculations were carried out at the minimum-energy geometries using analytical second derivatives. For the MP2 calculations with basis sets larger than 6-31+G(d,p), disk space limitations precluded such calculations. All calculations were performed using Gaussian98.[43]

3. Results and Discussion

3.1. Structures and Rotational Constants. For all methods and basis sets, the optimizations converged to a planar C_{2h} symmetric structure. The $(2\text{-pyridone})_2$ structure including the definitions of several geometry parameters is shown in Figure 1a. Figure 1b shows the close analogy to the hydrogen bonding

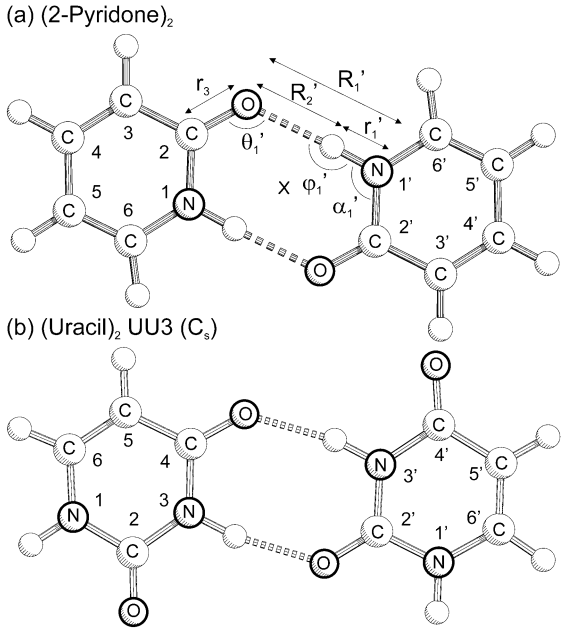

Figure 1. MP2/6-311++G(d,p) optimized structures of (a) $(2\text{-pyridone})_2$ and (b) the UU3 $(\text{uracil})_2$ isomer corresponding to the strongest bound biologically relevant uracil dimer. The definitions of structural parameters are employed in Table 1 and in the text.

pattern of the U·U isomer UU3,[15] also denoted HB3.[18] Table 1 characterizes the intramolecular and intermolecular bond lengths and angles associated with the N−H···O═C hydrogen bond. The experimentally determined angle θ_1(C═O···N) is 121.8 ± 0.5°.[32] Nearly all MP2 calculations predict θ_1 within this range, whereas the DFT methods predict 2−3° larger angles; see Table 1. The H-bond is predicted to be close to linear, φ(N−H···O) = 179° for all DFT and MP2 minimum energy structures; see Table 1.

In Figure 2, we plot the equilibrium rotational constants A_e, B_e, and C_e of $(2PY)_2$ vs the equilibrium R_e(N···O) distances, calculated with the methods and the basis sets indicated. Figure 2 also shows the experimental ground-state rotational constants A_0'', B_0'', and C_0'' determined by Held and Pratt; the experimental errors are ±0.1 MHz, about the width of the horizontal lines.[32] Using several model assumptions, Held and Pratt also determined a HB distance R_0(N···O) = 2.77 ± 0.03 Å from these data,[32] marked in Figure 2. Table 1 reports the rotational constants A_e, B_e, and C_e and their root-mean-square (RMS) deviations relative to experiment, ΔRMS, both absolute (MHz) and relative (%). With the MP2 method, the least good agreement overall is with the 6-31G*(0.25) basis set. For the seven basis sets studied, the smallest differences (ΔRMS = 1.4 MHz) are obtained with the 6-31+G(d,p) and 6-311++G(d,p) basis sets. The latter also yields the smallest relative RMS deviation of 0.3%. The MP2/6-31G(d,p) calculations yield almost exactly the experimental B and C, but a −13 MHz difference in A; the relative ΔRMS error is only 0.4%. The MP2 optimizations with the aug-cc-pVDZ and aug-cc-pVTZ basis sets yield B_e and C_e constants slightly larger than experiment, in agreement with the relatively short hydrogen bonds; see below. The MP2/aug-cc-pVTZ A_e constant is 10 MHz higher than the experimental A_0'', whereas the MP2/aug-cc-pVDZ A_e is 30 MHz lower, an unexpectedly large difference.

Turning to the DFT calculations, the B3LYP/6-311++G-(2d,2p) and PW91/6-311++G(d,p) calculations also yield very satisfactory B and C constants, but less good agreement with A. The absolute and relative ΔRMS errors are

TABLE 1: Calculated Structural Parameters (Ångstroms and Degrees) and Rotational Constants A_e, B_e, C_e (MHz) of the Fully Optimized Doubly N−H···O Hydrogen-Bonded (2-Pyridone)$_2$ Dimer and 2-Pyridone, with MP2, B3LYP, and PW91 Methods and Seven Different Basis Sets

		MP2							B3LYP		PW91
	exp[a]	A[b]	B	C	D	E	F	H	E	G	E
					(2-Pyridone)$_2$						
R_1(N···O)	2.77	2.721	2.729	2.752	2.744	2.735	2.710	2.723	2.780	2.768	2.730
r_1(N···H		1.065	1.051	1.040	1.043	1.044	1.054	1.044	1.040	1.039	1.059
r_3(C═O)		1.291	1.253	1.256	1.263	1.252	1.266	1.253	1.246	1.247	1.258
θ_1(C−O)···N)	121.8	122.8	121.9	121.5	122.7	122.9	121.6	122.7	124.3	123.2	123.0
A'', MHz	2014.4 ± 0.1	1956.7	1991.1	1997.6	2009.9	2012.5	1980.4	202.4	2022.8	2019.3	1998.2
B'', MHz	319.4 ± 0.1	311.9	318.9	319.3	317.5	318.4	320.6	322.6	312.8	316.1	318.0
C'', MHz	275.8 ± 0.1	269.0	274.2	275.3	274.2	274.9	275.9	278.5	270.9	273.3	274.3
ΔRMS, MHz		31.5	11.2	7.4	1.4	1.4	17.3	6.3	8.6	5.7	7.2
ΔRMS, %		2.5	0.7	0.4	0.5	0.3	0.9	0.9	1.6	0.8	0.5
					2-Pyridone						
A''	5643.758	5491.1	5632.0	5693.9	5676.5	5668.0	5660.4	5706.8	5660.4	5679.5	5626.6
B''	2793.471	2672.3	2747.1	2771.2	2768.2	2772.1	2739.7	2786.0	2787.4	2798.0	2759.4
C''	1868.823	1797.5	1846.5	1864.0	1860.8	1861.6	1840.4	1872.1	1867.7	1874.5	1851.4
ΔRMS, MHz		119.8	30.5	31.8	24.3	19.1	41.2	36.7	10.2	21.1	24.2
ΔRMS, %		3.7	1.2	0.7	0.7	0.6	1.5	0.7	0.2	0.4	0.9

[a] Reference 32. [b] Basis sets: A, 6-31G*(0.25);[18] B, cc-pVDZ; C, 6-31G(d,p); D, 6-31+G(d,p); E, 6-311++G(d,p); F, aVDZ; G, 6-311++G(2d,2p); H, aVTZ.

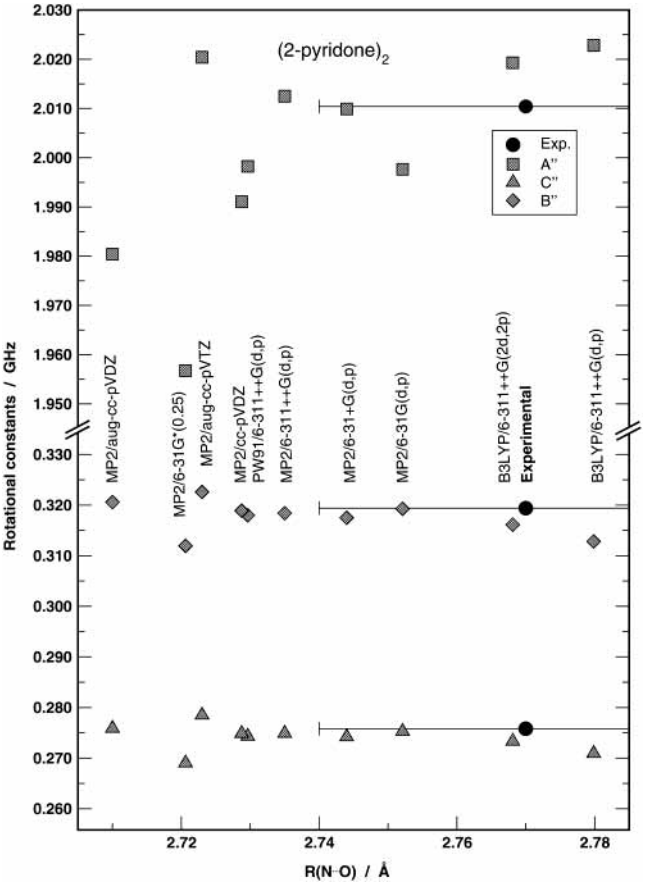

Figure 2. Calculated rotational constants A_e, B_e, and C_e of (2-pyridone)$_2$ vs the calculated hydrogen bond lengths R(N···O); see also Table 1. The experimental rotational constants A_0'', B_0'', and C_0'' (errors ±0.1 MHz) are plotted together with the experimental vibrationally averaged R_0(N···O) distance (±0.03 Å uncertainty).

comparable to those of the MP2/6-31G(d,p) and MP2/aug-cc-pVTZ calculations.

The experimental rotational constants and R_0(N···O) distance are zero-point (ZP) vibrationally averaged, whereas the calculated values are not. The deviations of the calculations should be expressed relative to A_e, B_e, and C_e rotational constants and R_e(N···O) derived from experiment, but these are not available.[32]

In perturbation-theoretical vibration−rotation interaction treatments, the ZP vibrational effects on the rotational constants consist of a positive "harmonic" contribution from all vibrations and a negative contribution from the cubic and higher terms of anharmonic vibrations (plus a contribution from degenerate vibrations to Coriolis coupling which is not relevant here).[44] It is not presently possible to include the effect of vibrational averaging of all 66 inter- and intramolecular modes using anharmonic potentials. We briefly consider the effects of the intermolecular vibrations, because these have the lowest frequencies and should contribute most to the ZP averaging effects: The out-of-plane vibrations ν_1 to ν_3 and the in-plane "opening" vibration ν_5 (discussed below) have potentials that are symmetric with respect to the vibrational displacements and are nearly perfectly harmonic, yielding dominantly harmonic contributions. The in-plane intermolecular vibrations ν_4 and ν_6 contribute to both the harmonic and to the anharmonic terms. Because there are six harmonic but only two anharmonic contributions, and because the out-of-plane vibrations have lower frequencies than the in-plane vibrations, the harmonic corrections should be larger than the anharmonic ones.[44] On the basis of the rotational constants and harmonic frequencies, we estimate the intermolecular vibrational ZP corrections[44] as $A_0 - A_e = +4$ to $+12$ MHz, $B_0 - B_e = +0.3$ to $+0.5$ MHz, and $C_0 - C_e = +0.15$ to $+0.25$ MHz. These estimates indicate that the calculated B_e and C_e values might be compared directly to experiment. As Table 1 indeed shows, the PW91 and all MP2 calculations except those with the 6-31G*(0.25) and aVTZ basis sets predict B_e and C_e rotational constants within 2 MHz of B_0 and C_0. However, the differences of the calculated A_e constants relative to A_0 are large, between $+13$ and -30 MHz; compensating for ZP averaging by the 8 ± 4 MHz indicted above does not improve agreement. Also, increasing the basis set size up to aVTZ with the MP2 method does not yet lead to a converged A_e value.

The intermolecular vibrational ZP averaging of rotational constants has been treated for several complexes and clusters by rigid body diffusion Monte Carlo methods.[45−56] However, these investigations concerned light molecules such as H_2 or H_2O with small masses, large rotational constants, and very large ZP amplitudes, also the hydrogen bond energies were typically

TABLE 2: MP2 Binding Energies of (2-Pyridone)$_2$ and (Formamide)$_2$ (kcal/mol) with the aug-cc-pVXZ (X = D, T, Q) Basis Sets and Extrapolation to the Complete Basis Set

	(2-pyridone)$_2$		(formamide)$_2$	
basis set	D_e	D_e^{CPC}	D_e	D_e^{CPC}
aug-cc-pVDZ	−24.735[a]	−20.996[a]	−15.597[b]	−12.759[b]
	(−24.637[b])	(−20.906[b])		
aug-cc-pVTZ	−23.854[a]	−21.984[a]	−16.087[b]	−14.470[b]
aug-cc-pVQZ	−23.240[a]	−22.359[a]	−15.916[b]	−15.107[b]
CBS limit[c]	−22.56[a]	−22.69[a]	−15.59[b]	−15.66[b]

[a] Computed at the aug-cc-pVTZ geometry. [b] Computed at the aug-cc-pVTZ geometry. [c] Extrapolation to the infinite basis set limit using the scheme of ref 57.

smaller than here. Thus the ZP effects calculated in those works are much larger than the corrections expected here.

As an estimate of the ZP vibrational averaging on the R_e(N···O) distance, we have calculated the effect on the intermolecular stretching vibration ν_6. In a one-dimensional pseudodiatomic approximation, and using the experimental harmonic frequency ω_e = 166.4 cm^{-1} and anharmonicity constant $\omega_e x_e$ = 1.4 cm^{-1} to determine an anharmonic Morse stretching potential,[13] we calculate $R_0 - R_e = +0.008$ Å for the ground vibrational state. The ν_4 in-plane shear vibration will lead to an increase of similar size. As noted above, the three out-of-plane modes and the in-plane ν_5 mode have nearly harmonic potentials, so they contribute only indirectly and should yield smaller increases of the hydrogen bond length. We estimate that the ZP averaging effect $R_0 - R_e$ due to the *inter* molecular modes is ≈+0.02 Å. As Figure 2 and Table 1 show, the MP2 as well as the PW91 methods predict R_e's in the range 2.72−2.75 Å, about 0.02−0.05 Å shorter than the experimental R_0 = 2.77 Å.[32]

The B3LYP/6-311++G(2d,2p) R(N···O) distance coincides with the experimental value of 2.77 Å, and the B3LYP/6-311++G(d,p) distance is 2.78 Å, just 0.01 Å longer (see Table 1 and Figure 2). This indicates that B3LYP may be effective for obtaining approximate vibrationally averaged HB distances; however, the MP2 and PW91 HB distances are physically more *correct*.

3.2. Binding Energies of (2-Pyridone)$_2$. *3.2.1 Complete Basis Set (CBS) Calculations on (2-Pyridone)$_2$ and (Formamide)$_2$.* The MP2 binding energies D_e and D_e^{CPC} of (2PY)$_2$ calculated with the aug-cc-pVXZ (X = D, T, Q) series are given in Table 2 and are plotted in the lower half of Figure 3. All values were calculated for the aug-cc-pVTZ optimized monomer and dimer geometries, the largest basis set for which we could perform complete structure optimization. The average of the CP-corrected and -uncorrected binding energies, $D_e^{1/2}$, as well as the Hartree−Fock contributions to the binding energies, D_e^{HF}, are also included in Figure 3.

We performed complete basis set (CBS) extrapolations of the binding energy, using the X = D, T, Q series and the extrapolation procedure of Klopper.[57] This yields $D_{e,CBS}$ = −22.56 kcal/mol using the CP-uncorrected D_e's; with the D_e^{CPC}'s we obtain $D_{e,CBS}^{CPC}$ = −22.69 kcal/mol, 0.13 kcal/mol larger than $D_{e,CBS}$. The CP-corrected and -uncorrected binding energies in Figure 3 are smaller and larger than $D_{e,CBS}$, as noted in other CBS studies on hydrogen-bonded systems,[2−4,6,58−62] but the opposite is true for the $D_{e,CBS}$ and $D_{e,CBS}^{CPC}$ limits. Figure 3 shows that the CP-corrected interaction energies converge more smoothly to the limit than the CP-uncorrected energies, as has been previously noted for smaller systems,[4−6,58,59] which may indicate that the $D_{e,CBS}^{CPC}$ limit is more reliable than the

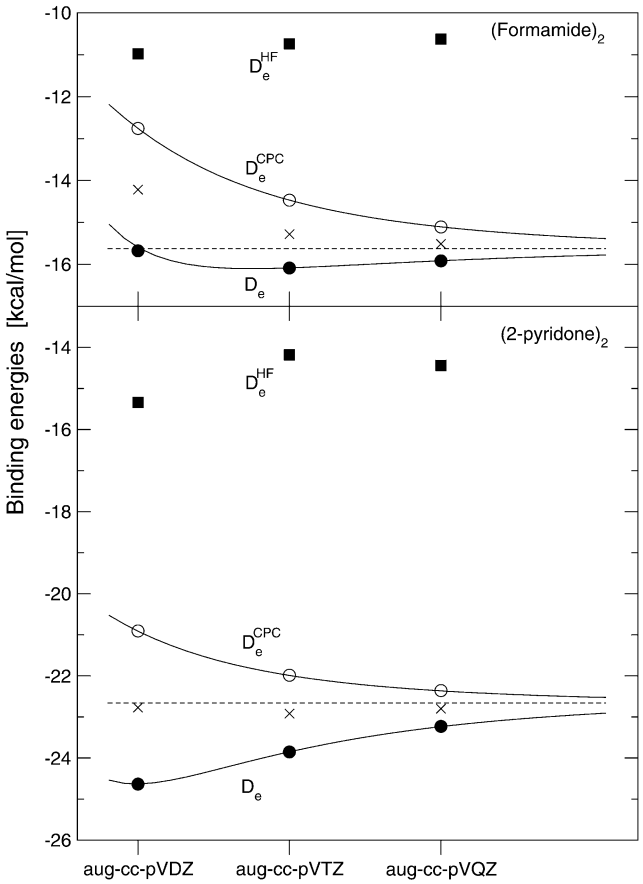

Figure 3. MP2 level complete basis set extrapolations for (2-pyridone)$_2$ and (formamide)$_2$, using the aug-cc-pVXZ (X = D, T, Q) basis sets: binding energies D_e (●) and counterpoise-corrected binding energies D_e^{CPC} (○) and average of the two, $D_e^{1/2}$ (×). The corresponding CBS limits are given by dashed lines.

$D_{e,CBS}$ value. The average binding energies $D_e^{1/2}$ lie close to the CBS limit for all three basis sets.

We performed an analogous CBS extrapolation study for the formamide dimer, (FA)$_2$, which exhibits the same antiparallel double N−H···O=C hydrogen-bond pattern as (2PY)$_2$.[61] To eliminate trivial differences between (FA)$_2$ and (2PY)$_2$ caused by geometry effects, we extracted the hydrogen-bonding part of the (FA)$_2$ geometries from the MP2/aug-cc-pVDZ geometries of 2PY and (2PY)$_2$ used above, optimizing only the two non-hydrogen-bonded C−H and N−H bonds that point away from the other dimer moiety. The CBS extrapolation of the D_e's lead to $D_{e,CBS}$ = −15.59 kcal/mol, that of the D_e^{CPC} values to a slightly larger value of $D_{e,CBS}$ = −15.66 kcal/mol. (These values *cannot* be directly compared to those of ref 61, because, there, the formamide dimer and monomer were fully structure optimized, giving a $D_{e,CBS}$ = −14.35 kcal/mol.)

Comparison of (FA)$_2$ with (2PY)$_2$ shows that the enlargement of the ring system increases the $D_{e,CBS}$ by 7.1 kcal/mol or 50%, from −15.6 to −22.7 kcal/mol. In Figure 3 we show the Hartree−Fock and MP2 binding energies separately. The CBS extrapolated Hartree−Fock binding energies of (FA)$_2$ and (2PY)$_2$ are −10.51 and −15.05 kcal/mol, respectively. Thus, in (FA)$_2$, about 4.6 kcal/mol or 30% of D_e and in (2PY)$_2$ about 7.6 kcal/mol or 33% of D_e is due to correlation, mainly long-range dispersive interactions and to a lesser extent to the change of intramonomer correlation energies upon dimerization. Of the 7.1 kcal/mol increase from (FA)$_2$ to (2PY)$_2$, 4.0 kcal/mol occurs at the Hartree−Fock level and is essentially due to electrostatic

and long-range inductive interactions, a 3.1 kcal/mol increase is due to the increase of dispersive interactions.

The $D_{e,CBS}$ of (2-pyridone)$_2$ dimer is also considerably larger than that of comparable doubly hydrogen-bonded dimers, such as the formamidine dimer $(H_2NCHNH)_2$,[21,60] the formic acid dimer $(HCOOH)_2$,[21,63,64] and the carbonic acid dimer $(HOCOOH)_2$.[63]

3.2.2. Higher Order Corrections. For the determination of accurate hydrogen bond interaction energies, higher order contributions to the correlation energy should be included. The CCSD(T) method provides very high accuracy, but due to the large size of $(2PY)_2$, CBS limit extrapolations at the CCSD(T) level were not feasible. Several authors have estimated the CCSD(T) CBS binding energy limit by adding to the MP2 CBS limit a correction term, $D_e^{CCSD(T)} - D_e^{MP2}$, which is evaluated with smaller basis sets than D_e^{MP2}.[5,21,23,59,65] The correction is typically ≈2−3% of D_e^{MP2} and usually decreases with increasing basis set size; both positive and negative corrections have been found. Thus, for the doubly hydrogen-bonded dimers (formic acid)$_2$, (formamide)$_2$, and (formamidine)$_2$, the $D_e^{CCSD(T)} - D_e^{MP2}$ corrections with the aug-cc-pVDZ basis set are 0.00, −0.06 and +0.63 kcal/mol, respectively.[21] Using CCSD(T) with the aug-cc-pVDZ basis set at the aug-cc-pVTZ optimized geometry, we obtain $D_e = -23.96$ kcal/mol, which amounts to a destabilizing correction of $D_e^{CCSD(T)} - D_e^{MP2} = +0.77$ kcal/mol or +3.1% of D_e^{MP2}. The size of the correction is in agreement with earlier findings, but the sign is opposite to that found for (formamide)$_2$, where −0.1 and −0.06 kcal/mol were calculated with the cc-pVTZ and aug-cc-pVDZ basis sets.[21] Combining the CCSD(T)/aug-cc-pVDZ correction with the MP2 CBS limit $D_{e,CBS}^{CPC} = -22.69$ kcal/mol yields an estimate of the CCSD(T) CBS limit of −21.92 kcal/mol.

In the MP2 and CCSD(T) aug-cc-pVXZ calculations the 1s orbitals on C, N, and O are not correlated (frozen core). The effect of correlating these core orbitals on the MP2 binding energies can be estimated from previous high-accuracy calculations[6,66] on $(H_2O)_2$ and $(H_2O)_3$, where increases of D_e by 0.02−0.04 kcal/mol per hydrogen bond were found upon including core correlation. The estimated correction for $(2PY)_2$ with two hydrogen bonds is −0.04 to −0.08 kcal/mol at the MP2 level.

We can now compare the magnitudes of the different corrections: (i) the finite size of the basis set leads to an uncertainty of the MP2 CBS extrapolation of 0.13 kcal/mol, (ii) the inclusion of core correlation in the MP2 calculation probably increases the D_e by about −0.06 kcal/mol, and (iii) the inclusion of higher order excitations at the CCSD(T) level decreases the binding energy by +0.77 kcal/mol, relative to the MP2 level. In contrast to similar analyses[6,66] on $(H_2O)_2$ and $(H_2O)_3$ we find that the higher order correlation energy contributions are the most significant correction, which may be due to the greater contribution of dispersion interactions in the (2-pyridone)$_2$ system.

3.2.3. Effects of Hydrogen Bonding on Electron Densities. The influence of hydrogen bonding on the electronic density $\rho(r)$ of HB donors and acceptors has been discussed by several authors.[67−71] Denoting the density of the 2PY monomer at point r by $\rho^0_{2PY}(r)$, the *difference density* between the dimer and the two monomers A and B is given by $\Delta\rho(r) = \rho_{(2PY)_2}(r) - \rho^0_{2PY,A}(r) - \rho^0_{2PY,B}(r)$. For these calculations, the geometries of the 2PY monomers are kept identical to that in the dimer. Figure 5 shows isosurface representations of the electronic density differences $\Delta\rho(r)$ of $(FA)_2$ and of $(2PY)_2$, both at contour values of ±0.004 au (1 atomic unit = 1 e$^-$ bohr^{-3}); the dark and light regions indicate loss and gain of electron density, respectively. Figure 6 shows a cut of $\Delta\rho(r)$ along one of the hydrogen bonds of $(2PY)_2$ in a contour representation. A number of interesting features are observed:

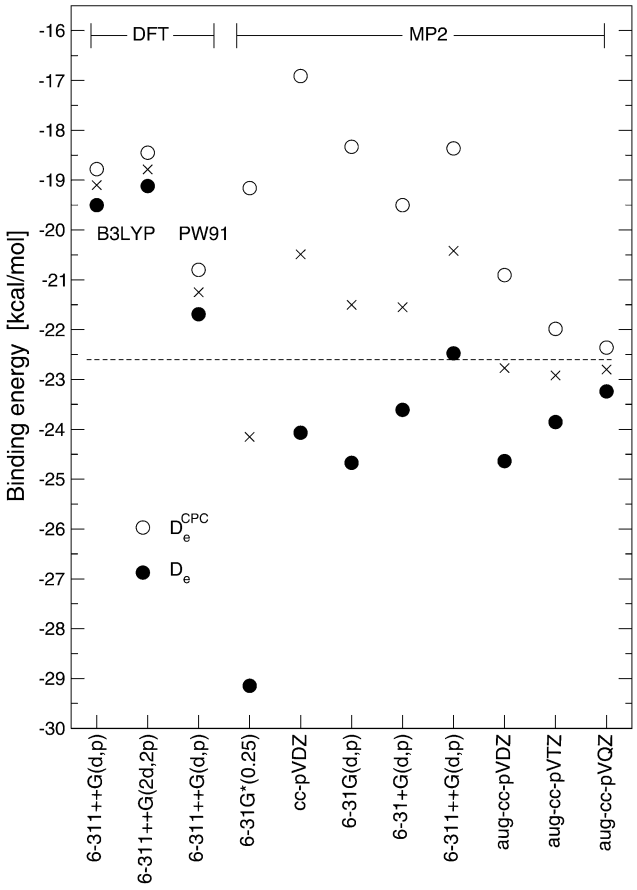

Figure 4. Binding energies D_e (●) and counterpoise-corrected binding energies D_e^{CPC} (○) of (2-pyridone)$_2$ and average of the two, $D_e^{1/2}$ (×), calculated with the B3LYP, PW91, and MP2 methods, using five different basis sets. The dashed line (- - -) corresponds to the MP2 CBS limit from Figure 3.

(i) At the N−H donor, the dominant effect of hydrogen bond formation is to displace electron density from the H atom into the N−H σ bond, close to the N atom. This has been previously interpreted as an effect of the mutual penetration of the H and O atoms.[69,70] At the N atom, Figures 5 and 6 reveal that density flows from the $2p_z$ orbital into the N−H σ bond relatively close to the N atom.

(ii) At the acceptor O atom, the opposite process occurs: σ-electron density close to the nucleus and oriented along the H bond flows into the oxygen $2p_z$ orbital. At the carbonyl C atom there is practically no electron rearrangement, note specifically the absence of any change of π-electron density. A small σ-electron flow occurs out of the C=O into the C−N bond. It has been generally noted that one of the features of H bonding is the lack of concentration of charge in the bonding region upon formation of the HB.[67−69] Also in other A−H···B hydrogen bonds, it has been noted that H loses electrons mainly to A, and to a much smaller extent to B.[69,70]

(iii) A small part of the electron density lost from the H atom flows to the bond critical point (BCP) near the center of the N−H···O H bond. In $(2PY)_2$, the maximum of $\Delta\rho(r)$ is 0.0056 au; compared to $\rho(r_{BCP}) = 0.0426$ au, the density difference amounts to a local increase of ≈13%.

(iv) The $\Delta\rho(r)$ plots of $(FA)_2$ and $(2PY)_2$ in Figure 5 are nearly identical. Even for much smaller density changes, the

TABLE 3: Experimental and Calculated Intermolecular Frequencies (cm^{-1}) of the Doubly N−H···O Hydrogen-Bonded (2-Pyridone) Dimer

			MP2				B3LYP		PW91
		exp[a]	A[b]	B	C	D	E	G	E
ν_1	buckle	22.3	22.3	18.7	21.0	8.9	30.3	29.8	26.5
ν_2	propeller twist	59.6	59.6	62.4	62.5	57.2	59.2	60.6	57.6
ν_3	stagger	89.8	97.5	99.8	99.5	75.8	92.4	92.4	94.0
ν_4	shear	98.09	8.1	100.3	102.0	100.9	103.2	104.0	104.6
ν_5	opening	107.9	117.0	111.5	107.4	108.3	105.7	107.3	112.3
ν_6	stretch	163.0	177.2	170.8	165.6	165.8	160.9	164.7	169.0
ΔRMS, cm^{-1} [c]		7.6	5.8	4.6	8.1		4.2	4.1	4.8
ΔRMS, %[d]		6.1	8.6	5.7	25.4	14.8		11.8	8.8

[a] Reference 33. [b] Basis sets: A, 6-31G*(0.25);[18] B, cc-pVDZ; C, 6-31G(d,p); D, 6-31+G(d,p); E, 6-311++G(d,p); G, 6-311++G(2d,2p). [c] Absolute root-mean square deviation. [d] Relative root-mean-square deviation.

TABLE 4: Calculated Binding Energies (kcal mol^{-1}) of the Doubly Hydrogen-Bonded (2-Pyridone)$_2$ Dimer, Using the MP2, B3LYP, and PW91 Methods and Eight Different Basis Sets[a]

	MP2							B3LYP		PW91
	A[a]	B	C	D	E	F	G	E	H	E
functs	216	246	260	316	378	412	874	378	478	378
D_e	−29.15	−24.07	−24.67	−23.61	−22.48	−24.64	−23.85	−19.50	−19.12	−21.69
BSSE	9.99	7.16	6.34	4.11	4.11	3.73	1.87	0.72	0.67	0.89
D_e^{CPC}	−19.16	−16.91	−18.33	−19.50	−18.36	−20.91	−21.98	−18.78	−18.45	−20.80
D_0	−28.20	−22.99	−23.48	−22.50				−18.33	−17.90	−20.86
ΔZPE_{dim}	0.95	1.08	1.19	1.11				−1.17	1.22	0.83
ZPE_{inter}	0.82	0.81	0.80	0.74				−0.79	0.80	0.81

[a] The vibrational zero-point energy, ΔZPE_{dim}, and intermolecular zero-point energy ZPE_{inter} are also given; see text. [b] Basis sets: A, 6-31G*(0.25);[18] B, cc-p-VDZ; C, 6-31G(d,p); D, 6-31+G(d,p); E, 6-311++G(d,p); F, aug-cc-pVDZ; G, aug-cc-pVTZ; H, 6-311++G(2d,2p).

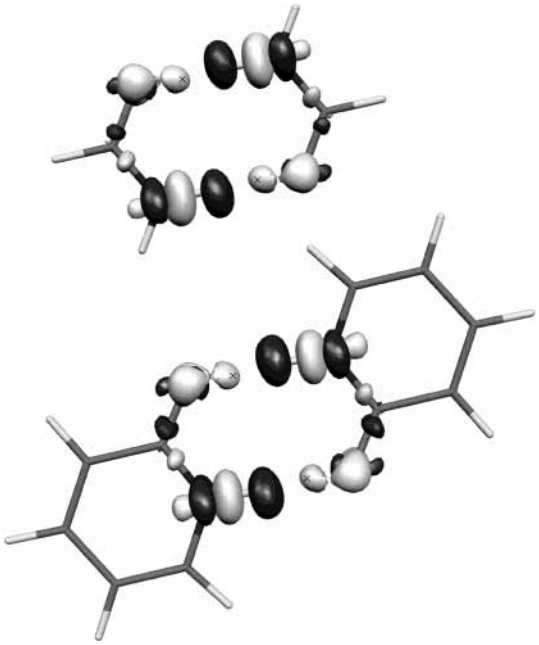

Figure 5. B3LYP/6-311++G(d,p) calculated difference densities $\Delta\rho$ of (a) the formamide dimer $(FA)_2$, (b) the 2-pyridone dimer $(2PY)_2$, at an isosurface value of ±0.004 atomic units ($e^-/bohr^{-3}$). The center of the H···O distance is marked by ×.

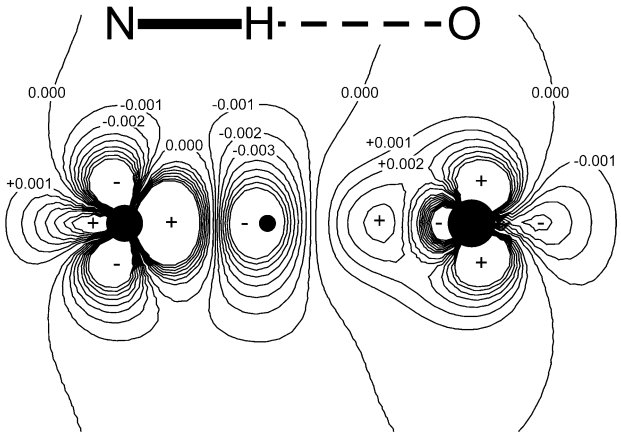

Figure 6. B3LYP/6-311++G(d,p) calculated difference densities $\Delta\rho$ along the hydrogen bond of the 2-pyridone dimer $(2PY)_2$, in a contour representation. The contour spacings are 0.001 $e^-/bohr^3$.

electron density redistributions of $(FA)_2$ and $(2PY)_2$ are very similar. We conclude that the extension of the molecular framework in the O═C−N π-electron system in $(FA)_2$ to the entire aromatic framework in $(2PY)_2$ does not lead to additional electron flow into or out of the hydrogen bonding region. This is in contrast to the expectations of "resonance enhancement" of hydrogen bonds.[72,73] It is also difficult to interpret the 50% larger HB binding energy of $(2PY)_2$ relative to $(FA)_2$ in terms of the electron density redistributions shown in Figure 5, emphasizing the importance of the dispersive interactions.

3.2.4. Basis Set Dependence of Binding Energies of (2-Pyridone)$_2$. Using the MP2 binding energy limit of $(2PY)_2$ discussed above, we compare the performance (i) of different correlated methods and (ii) of the MP2 method using different basis sets. The motivation for this investigation is that very large basis sets lead to prohibitively long computational times for systems that either have no symmetry and/or involve larger subunits such as nucleobases, and also for vibrational frequencies or thermodynamic properties that are expensive to calculate. Figure 4 gives an overview of all the D_e and D_e^{CPC} values calculated with different correlated methods and basis sets. For the smaller basis sets up to 6-31+G(d,p) the harmonic vibrational frequencies and the dissociation energies D_0 could be calculated. The detailed D_e, D_e^{CPC}, and D_0 values are given in Table 4.

The MP2 calculations give larger binding energies which lie in the range $D_e = -22$ to -29 kcal/mol. Compared to the DFT methods, the MP2 method is afflicted by relatively large BSSEs,

especially for the smaller basis sets: the 6-31G*(0.25) basis set, which has been used for extensive studies of nucleic acid dimers[18] has a BSSE of about 10 kcal/mol and the cc-pVDZ basis set 7.2 kcal/mol.

As Figure 4 shows, for many basis sets the CP-uncorrected D_e is much closer to $D_{e,CBS}$ than the CP-corrected D_e^{CPC}. An important finding is that the CP-uncorrected D_e's of medium-size basis sets such as 6-31+G(d,p) or 6-311++G(d,p) that allow structure optimizations and vibrational normal-mode calculations differ by only ±1 kcal/mol or less than ±5% from the $D_{e,CBS}$ value. Even with the large aug-cc-pVXZ (X = D, T, Q) basis sets the CP-uncorrected MP2 binding energies are very close to the CBS value for $(FA)_2$; for $(2PY)_2$ the CP-corrected and -uncorrected D_e's bracket the CBS value nearly equally; see Figure 3. For this reason we give the CP-uncorrected dissociation energies D_0 in Table 4.

For all DFT calculations the BSSEs are small (0.7−0.9 kcal/mol), corresponding to only 3−4% of the uncorrected binding energy D_e. The B3LYP density functional method yields D_e's of −19.2 to −19.5 kcal/mol, the smaller basis set leading to the larger binding energy. With the PW91 method and the 6-311++G(d,p) basis, the D_e is −21.7 kcal/mol, 2.3 kcal/mol or 12% larger than with the B3LYP method, and in excellent agreement with the estimated CCSD(T) CBS limit of −21.9 kcal/mol. Tsuzuki and Lüthi have shown that for hydrogen-bonded systems the PW91 functional yields improved binding energies compared to B3LYP (and other) density functionals.[39] Because the PW91/6-311++G(d,p) calculation combines a very good D_e with low BSSE, it is no surprise that the optimized minimum-energy structure also yields a very good HB distance; see above.

3.3. Intermolecular Vibrational Frequencies. Table 3 gives the calculated intermolecular frequencies for $(2PY)_2$. These differ slightly from the experimental frequencies due to diagonal anharmonicity and off-diagonal (intermode) couplings. The experimental intermolecular frequencies of $(2PY)_2$ were reported in refs 13 and 33 and are also given in Table 3. For the experimentally measured in-plane shear (ν_4) and stretch (ν_6) modes, the diagonal anharmonicities are ≈0.2 and 1.4 cm^{-1}, respectively. As discussed above, the potential energy curves along the ν_1 to ν_3 out-of-plane and the in-plane ν_5 vibrational coordinates are nearly harmonic. In Table 3, we give both the absolute and relative root-mean-square deviations ΔRMS between the harmonic and experimental frequencies.

The B3LYP harmonic frequencies provide the best *effective* predictions of the experimental fundamental frequencies, yielding ΔRMS = 4.2 cm^{-1} and 4.5%, respectively. The main contribution to the RMS deviations is from the ν_1 "buckle" mode, which is calculated 8 cm^{-1} or 30% too high compared to the experimental value; the other deviations are <5%. The PW91 intermolecular frequencies are slightly higher than the B3LYP frequencies, as would be expected from the higher D_e of the PW91 calculation. The overall agreement for PW91 is very satisfactory, the only exception being again the ν_1 buckle frequency which is calculated 4 cm^{-1} or 16% too high.

The MP2/6-31G(d,p) combination exhibits the smallest overall relative deviation; see Table 3. Compared to B3LYP, the absolute and relative deviations of the ν_1 "buckle" mode are much smaller, and the ν_4 and ν_6 harmonic frequencies agree almost quantitatively with experiment.[33] The other intermolecular frequencies are reproduced to <5%, with the exception of the ν_3 "stagger" mode where the MP2 frequency is 10 cm^{-1} or 12% above experiment. The MP2/6-31+G(d,p) calculation also gives good results, with the exception of the ν_1 mode; see Table 3.

TABLE 5: MP2-Calculated Standard Enthalpies $\Delta_{dim}H°$, Entropies $\Delta_{dim}S°$, and Free Energies $\Delta_{dim}G°$ for the Dimerization of 2-Pyridone at T = 298.15 K, with the 6-31G(d,p) and 6-31+G(d,p) Basis Sets[a]

basis set	6-31G(d,p)	6-31+G(d,p)
$\Delta_{dim}H°$, kcal/mol	−23.30	−22.20
$\Delta_{dim}S°$, cal/(mol deg)	−38.64	−35.15
$\Delta_{dim}G°$, kcal/mol	−11.78	−11.72
q_{rot}	1.036×10^6	1.037×10^6
q_{vib}	1.183×10^4	5.402×10^4

[a] Also given are the rotational and vibrational contributions to the dimer partition function.

On the basis of the harmonic frequencies, the vibrational ZP change upon dimerization, $\Delta ZPE_{dim} = ZPE_{dim} - 2ZPE_{mon}$, were evaluated. Those MP2 and B3LYP calculations that give the best agreement with experiment predict ΔZPE_{dim} = 1.1−1.2 kcal/mol, which is about 5% of the binding energy $D_{e,CBS}$. The ZPE change can be further divided into the contribution of the six intermolecular modes to ZPE, ZPE_{inter}, and the changes of the monomer ZPE, ΔZPE_{intra}, resulting from the intramolecular vibrational frequency *changes* upon dimer formation. ZPE_{inter} is consistently calculated to be 0.8 kcal/mol or about two-thirds of the total ZPE change upon dimerization.

3.4. Gas-Phase Dimer Equilibrium. Using the rotational constants and harmonic vibrational frequencies from the structure and vibrational calculations, the standard enthalpies $\Delta_{dim}H°$, entropies $\Delta_{dim}S°$, and free energies $\Delta_{dim}G°$ of the dimerization 2PY(g) + 2PY(g) → $(2PY)_2$(g) were calculated at the MP2/6-31G(d,p) and 6-31+G(d,p) levels in the rigid-rotor/harmonic-oscillator approximation at 298.15 K and are given in Table 5. The standard dimerization enthalpies $\Delta_{dim}H°$ are −23.30 and −22.20 kcal/mol, respectively. The standard entropies of dimerization, $\Delta_{dim}S°$, differ by 3.5 cal/(mol deg) or 10%, a comparatively large amount. The translational partition functions do not contribute to this difference, because they depend only on mass and temperature and not on the ab initio method. The rotational constants and partition functions calculated with both methods lie within 0.6% for $(2PY)_2$ and within 0.3% for the 2PY monomer (see Table 1), so the rotational contribution to the difference is small. The difference of $\Delta_{dim}S°$ can be traced to the contributions of the low-frequency vibrations that are thermally excited at 298 K: In Table 3 we notice the large frequency differences for the ν_1 buckle and the ν_3 stagger intermolecular vibrations. Indeed, the vibrational dimer partition functions calculated with the different basis sets differ by a factor of 4.6, as shown in Table 5. This shows that a exact knowledge of the low-frequency vibrations is of fundamental importance for thermodynamic considerations.

The standard free energy of dimerization $\Delta_{dim}G°$ is −11.78 at the MP2/6-31G(d,p) and −11.72 kcal/mol at the MP2/6-31+G(d,p) levels; see Table 5. The close agreement is due to a fortuitous cancellation of the 1 kcal/mol difference of $\Delta_{dim}H°$ and of the $T\Delta_{dim}S°$ factor at 298 K. Clearly, the gas-phase dimerization equilibrium lies completely on the dimer side.

In the gas phase, the 2-pyridone monomer also exists in the enol or 2-hydroxypyridine (2HP) form. The gas-phase enol: keto tautomer ratio has been measured[74] to be 2HP:2PY = 3:1, thus 2HP is actually the major tautomer. A complete description of the gas-phase equilibria would involve the 2HP ↔ 2PY tautomerization and the three dimerization equilibria 2PY + 2PY → $(2PY)_2$, 2PY + 2HP → 2PY·2HP, and 2HP + 2HP → $(2HP)_2$ and is outside the scope of this work.

3.5. Overall Considerations. For the rotational constants, good overall agreement was found using the MP2 method and basis sets 6-31G(d,p) or larger. On the other hand, the MP2/6-31G*(0.25) basis set combination, which was developed for BSSE-corrected single points and was never intended to use for optimizations, clearly should not be used for structure optimizations or calculations of properties at those stationary points. The best agreement with the experimental rotational constants was found with the 6-31+G(d,p) and 6-311++G-(d,p) basis sets. The aug-cc-pVDZ basis set, which predicts excellent *B* and *C* constants, leads to an unexpectedly large deviation of −30 MHz or −1.5% in *A*. This can be traced to the deviations of the *monomer B* constant (correlating with the dimer *A* constant) with the MP/aug-cc-pVDZ basis set. For those MP2 calculations that show <8 MHz RMS absolute deviation from the experimental rotational constants, the calculated HB distances vary over the range $R_e(N\cdots O) = 2.72-2.75$ Å. The highest level MP2/aug-cc-pVTZ calculation yields $R_e(N\cdots O) = 2.723$ Å, at the low end of this range.

Of the two density functional methods tested, the PW91/6-311++G(d,p) predictions of rotational constants and hydrogen bond distance are very good, comparable to those of the more accurate MP2 calculations. The B3LYP calculations are in less good agreement with experiment than the PW91 method.

For the binding energy our point of reference is given by the CBS extrapolated MP2 limits, −22.62 ± 0.07 kcal/mol. The CP-uncorrected MP2 binding energies with medium-sized basis sets such as 6-31+G(d,p) and 6-311++G(d,p) are close to this value, due to a compensation of the basis set incompleteness and basis set superposition errors. Similar good agreement is found also for the CP-uncorrected PW91/6-311++G(d,p) calculation.

The B3LYP calculations predict D_e's that are 15−17% too low, similar to the experience reported by Tsuzuki and Lüthi. The B3LYP rotational constants are comparable to the PW91 and the better MP2 values. The H bond distances are 0.03−0.05 Å too long but turn out to be in agreement with the experimental vibrationally averaged values. The B3LYP harmonic frequencies show good agreement with experiment.

In terms of computational cost and overall agreement with experiment, the MP2/6-31+G(d,p) combination turns out to be extremely effective. Currently it is probably the limit for MP2 vibrational calculations on systems of this size. To obtain significantly better predictive capability, one needs to use at least aug-cc-pVTZ, a 3 times larger basis set. The PW91/6-311++G(d,p) combination is seen to provide results in agreement with the best MP2 methods at even lower cost; it is to be preferred over the B3LYP method, except for vibrational frequencies.

4. Conclusions

The structures, rotational constants, intermolecular vibrational frequencies, and binding energies of $(2\text{-pyridone})_2$ were investigated by the correlated MP2 method and the B3LYP and PW91 density functionals. For the MP2 method, a wide range of split-valence basis sets with and without diffuse functions up to the large augmented correlation-consistent basis sets was used. By comparison to the experimental data, the quality of the three different methods and of the different basis sets could be established for this important model dimer with respect to the different properties, i.e., structure, rotational constants, vibrations, and binding energies.

Full structure optimizations of $(2\text{-pyridone})_2$ were carried out at the MP2 level with basis sets up to aug-cc-pVTZ. With the latter, the MP2 optimized $R_e(N\cdots O)$ is 2.723 Å. We estimate that extrapolation to complete basis set and including higher order correlation energy at the CCSD(T) level to lengthen the $R_e(N\cdots O)$ by 0.02−2.74 Å. The intermolecular vibrational averaging effects are estimated to increase the H bond distance by another 0.04 Å, to $R_0 \approx 2.78$ Å. The latter value is in very good agreement with the vibrationally averaged $R_0(N\cdots O) = 2.77$ Å obtained by Held and Pratt.[32] At the MP2 level, the smaller 6-31+G(d,p) and 6-311++G(d,p) basis sets predict $R_e(N\cdots O)$ values in the range 2.735−2.745 Å, in excellent agreement with the estimated CBS limit for $R_e(N\cdots O)$. The PW91 density functional with the 6-311++G(d,p) basis set also yields a very good $R_e(N\cdots O) = 2.730$ Å, whereas the B3LYP functional predicts $R_e(N\cdots O) = 2.78$ Å which is about 0.05 Å too long.

The experimental rotational constants of $(2PY)_2$ are best reproduced at the MP2 level with the 6-31+G(d,p) and 6-311++G(d,p) basis sets. All the MP2 and DFT calculations with medium and large basis sets reproduce the *B* and *C* rotational constants to ≤0.5%, but the agreement in the *A* constant is only ±1−2%. The differences are especially large for the MP2/aug-cc-pVDZ and aug-cc-pVTZ calculations.

Using the aug-cc-pVXZ (X = D, T, Q) basis sets with the CBS extrapolation procedure,[57] the MP2 binding energy limit is extrapolated as $D_{e,CBS} = -22.62 \pm 0.07$ kcal/mol. The MP2/6-311++G(d,p) calculation that was shown to yield an excellent $R_e(N\cdots O)$ predicts a binding energy −22.48 kcal/mol, in very good agreement with the MP2 CBS limit. A further correction for higher order correlation energy at the CCSD(T) level was determined, which reduces the binding energy by +0.77 kcal/mol or +3.1%, yielding an estimate of the CCSD(T) CBS limit of −21.92 kcal/mol. This is the largest accurate binding energy calculated for a doubly hydrogen-bonded gas-phase dimer so far.

For the formamide dimer with the same hydrogen bond geometry, the CBS extrapolation yields $D_{e,CBS} = -16.63 \pm 0.04$ kcal/mol, which is 26% smaller than the binding energy of $(2\text{-pyridone})_2$. The 6 kcal/mol difference can be traced to the larger in-plane inductive and dispersive interactions of the 2-pyridone molecule.

The CP-uncorrected PW91/6-311++G(d,p) and MP2/6-311++G(d,p) binding energies are very close to the limiting value within the error estimate. Because both methods also provide rotational constants and hydrogen bond lengths that are very close to the observed values, we find them to be extremely effective estimators for the CBS structures and binding energies of this model dimer. For the intermolecular vibrations, the B3LYP method is the most effective predictor method.

Acknowledgment. This work was supported by the Schweiz. Nationalfonds (project no. 2000-68081.02) and by the Swiss supercomputing center CSCS in Manno.

References and Notes

(1) Feller, D. *J. Chem. Phys.* **1992**, *96*, 6104.

(2) Peterson, K. A.; Dunning, T. H., Jr. *J. Chem. Phys.* **1995**, *102*, 2032.

(3) Feyereisen, M. W.; Feller, D.; Dixon, D. A. *J. Phys. Chem.* **1996**, *100*, 2993.

(4) Xantheas, S. S. *J. Chem. Phys.* **1996**, *104*, 8821.

(5) Halkier, A.; Koch, H.; Jorgensen, P.; Christiansen, O.; Nielsen, I. M. B.; Helgaker, T. *Theor. Chem. Acta* **1997**, *97*, 150.

(6) Schütz, M.; Brdarski, S.; Widmark, P.-O.; Lindh, R.; Karlström, G. *J. Chem. Phys.* **1997**, *107*, 4597.

(7) Dunning, T. H.; Peterson, K. A.; van Mourik, T. In *Recent Theoretical and Experimental Advances in Hydrogen Bonded Clusters*;

Xantheas, S. S., Ed.; NATO ASI Series C; Kluwer Academic: Dordrecht, The Netherlands, 2000.
(8) Gu, J.; Leszczynski, J. *J. Phys. Chem. A* **2000**, *104*, 1898.
(9) Gu, J.; Leszczynski, J. *J. Phys. Chem. A* **2000**, *104*, 7353.
(10) Nir, E.; Janzen, C.; Imhof, P.; Kleinermanns, K.; de Vries, M. S. *Phys. Chem. Chem. Phys.* **2002**, *4*, 740.
(11) Nir, E.; Janzen, C.; Imhof, P.; Kleinermanns, K.; de Vries, M. S. *Phys. Chem. Chem. Phys.* **2002**, *4*, 732.
(12) Plutzer, C.; Hunig, I.; Kleinermanns, K. *Phys. Chem. Chem. Phys.* **2003**, *5*, 1158.
(13) Müller, A.; Talbot, F.; Leutwyler, S. *J. Chem. Phys.* **2000**, *112*, 3717.
(14) Müller, A.; Talbot, F.; Leutwyler, S. *J. Chem. Phys.* **2001**, *115*, 5192.
(15) Hobza, P.; Šponer, J. *Chem. Rev.* **1999**, *99*, 3247.
(16) Šponer, J.; Leszczynski, J.; Hobza, P. *J. Chem. Phys.* **1996**, *100*, 1965.
(17) Šponer, J.; Leszczynski, J.; Hobza, P. *J. Phys. Chem.* **1996**, *100*, 5590.
(18) Kratochvil, M.; Engkvist, O.; Šponer, J.; Jungwirth, P.; Hobza, P. *J. Phys. Chem. A* **1998**, *102*, 6921.
(19) Hobza, P.; Šponer, J. *Chem. Phys. Lett.* **1998**, *288*, 7.
(20) Jurečka, P.; Nachtigall, P.; Hobza, P. *Phys. Chem. Chem. Phys.* **2001**, *3*, 4578.
(21) Jurečka, P.; Hobza, P. *Chem. Phys. Lett.* **2002**, *365*, 89.
(22) Hobza, P.; Šponer, J. *J. Am. Chem. Soc.* **2002**, *124*, 11802.
(23) Leininger, M. L.; Nielsen, I. M. B.; Colvin, M. E.; Janssen, C. L. *J. Phys. Chem. A* **2002**, *106*, 3850.
(24) Baeyends, K. J.; Bondt, H. L. D.; Holbrook, S. R. *Nat. Struct. Biol.* **1995**, *2*, 52.
(25) Sukhodub, L. F.; Yanson, I. K. *Nature* **1976**, *264*, 247.
(26) Yanson, I. K.; Teplitzky, A. B.; Sukhodub, L. F. *Biopolymers* **1979**, *18*, 1149.
(27) Sukhodub, L. F. *Chem. Rev.* **1987**, *87*, 589.
(28) Brameld, K.; Dasgupta, S.; Goddard, W. A. *J. Phys. Chem. B* **1997**, *101*, 4851.
(29) Kabelač, M.; Hobza, P. *J. Phys. Chem. B* **2001**, *105*, 5804.
(30) Ryjacek, F.; Engkvist, O.; Vacek, J.; Kratochvil, M.; Hobza, P. *J. Phys. Chem. A* **2001**, *105*, 1197.
(31) Held, A.; Champagne, B. B.; Pratt, D. *J. Chem. Phys.* **1991**, *95*, 8732.
(32) Held, A.; Pratt, D. *J. Chem. Phys.* **1992**, *96*, 4869.
(33) Müller, A.; Talbot, F.; Leutwyler, S. *J. Chem. Phys.* **2002**, *116*, 2836.
(34) Fujimaki, E.; Fujii, A.; Ebata, T.; Mikami, N. *J. Chem. Phys.* **2000**, *112*, 137.
(35) Matsuda, Y.; Ebata, T.; Mikami, N. *J. Chem. Phys.* **2000**, *113*, 573.
(36) Dunning, T. H., Jr. *J. Chem. Phys.* **1989**, *90*, 1007.
(37) Kendall, R. A.; Dunning, T. H., Jr.; Harrison, R. J. *J. Chem. Phys.* **1992**, *96*, 6796.
(38) Woon, D. E.; Dunning, T. H., Jr. *J. Chem. Phys.* **1993**, *98*, 1358.
(39) Tsuzuki, S.; Lüthi, H. *J. Chem. Phys.* **2001**, *114*, 3949.
(40) Rabuck, A. D.; Scuseria, G. E. *Theor. Chem. Acc.* **2000**, *104*, 439.
(41) Boys, S. F.; Bernardi, F. *Mol. Phys.* **1970**, *19*, 553.
(42) van Duijneveldt, F. B.; van Duijneveldt-van de Rijdt, J. G. C. M.; van Lenthe, J. H. *Chem. Rev.* **1994**, *94*, 1873.
(43) Frisch, M. J.; Trucks, G. W.; Schlegel, H. B.; et al. *Gaussian 98*, Revision A.11.A; Gaussian, Inc.: Pittsburgh, PA, 1998.
(44) Kroto, H. *Molecular Rotation Spectra*; Dover Publications: Mineola, NY, 1992.
(45) Buch, V. *J. Chem. Phys.* **1992**, *97*, 726.
(46) Sandler, P.; Jung, J. O.; Szczesniak, M. M.; Buch, V. *J. Chem. Phys.* **1994**, *101*, 1378.
(47) Gregory, J. K.; Clary, D. C. *Chem. Phys. Lett.* **1994**, *228*, 547.
(48) Gregory, J. K.; Clary, D. C. *J. Chem. Phys.* **1995**, *102*, 7817.
(49) Gregory, J. K.; Clary, D. C. *J. Chem. Phys.* **1995**, *103*, 8924.
(50) Gregory, J. K.; Clary, D. C. *J. Chem. Phys.* **1996**, *105*, 6626.
(51) Gregory, J. K.; Clary, D. C. *J. Phys. Chem.* **1996**, *100*, 18014.
(52) Sandler, P.; Buch, V.; Sadlej, J. *J. Chem. Phys.* **1996**, *105*, 10387.
(53) van Mourik, T.; Benoit, D. M.; Price, S. L.; Clary, D. C. *Phys. Chem. Chem. Phys* **2000**, *2*, 1281.
(54) Shuler, K.; Dykstra, C. E. *J. Phys. Chem. A* **2000**, *104*, 4562.
(55) Shuler, K.; Dykstra, C. E. *J. Phys. Chem. A* **2000**, *104*, 11522.
(56) Arunan, E.; Emilsson, T.; Gutowsky, H. S.; Dykstra, C. E. *J. Chem. Phys.* **2001**, *114*, 1242.
(57) Klopper, W. *J. Chem. Phys.* **1995**, *102*, 6168.
(58) Stalring, L.; Schütz, M.; Lindh, R.; Karlstrom, G.; Widmark, P.-O. *Mol. Phys.* **2002**, *100*, 3389.
(59) Klopper, W.; Lüthi, H. P. *Mol. Phys* **1999**, *96*, 559.
(60) Šponer, J.; Hobza, P. *J. Phys. Chem. A* **2000**, *104*, 4592.
(61) Vargas, R.; Garza, J.; Friesner, R. A.; Stern, H.; Hay, B. P.; Dixon, D. A. *J. Phys. Chem. A* **2001**, *105*, 4963.
(62) Xantheas, S. S.; Burnham, C. J.; Harrison, R. *J. Chem. Phys.* **2002**, *116*, 1493.
(63) Liedl, K. R.; Sekusak, S.; Mayer, E. *J. Am. Chem. Soc.* **1997**, *119*, 3782.
(64) Chocholousova, J.; Vacek, J.; Hobza, P. *Phys. Chem. Chem. Phys.* **2002**, *4*, 2119.
(65) Tsuzuki, S.; Honda, K.; Uchimaru, T.; Mikami, M.; Tanabe, K. *J. Phys. Chem. A* **1999**, *103*, 8265.
(66) Nielsen, I. M. B.; Seidl, E. T.; Janssen, C. L. *J. Chem. Phys.* **1999**, *110*, 9435.
(67) Bader, R. F. W. *Atoms in Molecules. A Quantum Theory*; Clarendon: Oxford, U.K., 1990.
(68) Arnold, W. D.; Oldfield, E. *J. Am. Chem. Soc.* **2000**, *122*, 12835.
(69) Galvez, O.; Gomez, P. C.; Pacios, L. F. *J. Chem. Phys.* **2001**, *115*, 11166.
(70) Galvez, O.; Gomez, P. C.; Pacios, L. F. *J. Chem. Phys.* **2003**, *118*, 4878.
(71) Coussan, S.; Manca, C.; Tanner, C.; Bach, A.; Leutwyler, S. *J. Chem. Phys.* **2003**, *119*, 3774.
(72) Gilli, G.; Bellucci, F.; Ferretti, V.; Bertolasi, V. *J. Am. Chem. Soc.* **1989**, *111*, 1023.
(73) Gilli, G.; Bertolasi, V.; Ferretti, V.; Gilli, P. *Acta Crystallogr. B* **1993**, *49*, 564.
(74) Hatherley, L. D.; Brown, R. D.; Godfrey, P. D.; Pierlot, A. P.; Caminati, W.; Damiani, D.; Melandri, S.; Favero, L. B. G. *J. Phys. Chem.* **1993**, *97*, 46.